PCCP

ARTICLE

Photoluminescent Properties of Self-Assembled Chitosan-Based Composites Containing Semiconductor Nanocrystals†

Received 00th January 20xx,
Accepted 00th January 20xx

DOI: 10.1039/x0xx00000x

www.rsc.org/

Nina Slyusarenko,*[a] Marina Gerasimova [a] , Alexei Plotnikov [b] , Nikolai Gaponik [c] and Evgenia Slyusareva [a]

Photoluminescent (PL) properties of composites obtained by embedding of green-emitted semiconductor nanocrystals (NCs) of two different types (thiol-capped CdTe and CdSe/ZnS) into the chitosan-based biopolymer particles were investigated. The synthesis of self-assembled particles from oppositely charged polysaccharides involved a preliminary electrostatic binding of positively charged chitosan chains by negatively charged functional groups of NCs stabilizing ligand. The amount of NCs and the acidity of the solution were found to be important parameters influencing the PL. The PL properties were mainly discussed in terms of the colloidal stability of the particles and changes in energy gap of NCs. Generally, the obtained biocompatible composites with NCs randomly distributed within a biopolymer particle demonstrated a higher PL resistance to the solution acidity that expands the applicability range of thiol-capped NCs.

Introduction

Tunable optical and electronic properties of semiconductor nanocrystals (NCs) due to a size-dependent band gap allows fabrication of photoluminescent materials with predetermined properties covering a wide application range. Thus, the use of NCs as luminophores for immunoassays instead of traditional organic dyes significantly improves the sensitivity of the method;[1] the narrow band light emission from NCs considerably broadens the color gamut of NC-based LED displays.[2] However, the utility of water-soluble NCs is typically limited unless they are functionalized with organic molecular ligands. Functionalization improves solubility, colloidal stability and biocompatibility of NCs making them building blocks for engineering of various composites for numerous applications in modern photonics.

Conjugates of semiconductor nanocrystals as highly efficient luminophores with biopolymers as stabilizing and environment-responsive materials are the subject of intensive study over the last decades. Composites containing ensembles of NCs draw much attention due to cooperative effects (e.g., Förster's resonant energy transfer, FRET[3,4]) as well as their suitability for single-molecule spectroscopy.[5,6]

Stability of photoluminescent properties of NCs is of a great importance for biological applications of NC-based materials as the parameters of physiological media (e.g., pH, ionic strength) may significantly deviate from the values being optimal for the NC-performance. Thus, proper conjugation of NCs with additional stabilizing organic ligands plays crucial role for the applicability of NCs under unfavorable environmental conditions. In particular, functionalization with polymers enables the use of NCs as fluorophores for intracellular visualization[7], in the gastrointestinal tract with strongly acid conditions (pH 1-2)[8] and in urine samples.[9]

In the present work fluorescent composites from polysaccharide molecules and thiol-capped NCs were fabricated in an aqueous solution in order to develop a robust photoluminescent system suitable for biomarker and biosensor-based applications. Two different types of semiconductor NCs – core only CdTe synthesized in water and core-shell CdSe/ZnS synthesized in organic media, both with peak emission of about 530 nm – were used as luminophores. The composites (particles) were formed by self-assembling of two oppositely charged natural polyelectrolytes chitosan and chondroitin sulfate accompanied by the additional linking of charged functional groups of NCs ligands. The morphology of the synthesized composites as well as PL properties of NCs embedded into biopolymer particles were studied in depths and compared with those for NCs dispersed in water. PL properties of composites are discussed in terms of colloidal stability and changes in electron structure of NCs. The obtained NCs-containing particles were examined within a wide range of HCl concentration demonstrating their significantly improved resistance to degradation.

[a] Siberian Federal University, Svobodny Prospect 79, 660041 Krasnoyarsk, Russia.
[b] Freiberger Compound Materials GmbH, Am Junge-Löwe-Schacht 5, 09599 Freiberg, Germany.
[c] Technische Universität Dresden, 01062 Dresden, Germany.

†Electronic Supplementary Information (ESI) available. See DOI: 10.1039/x0xx00000x

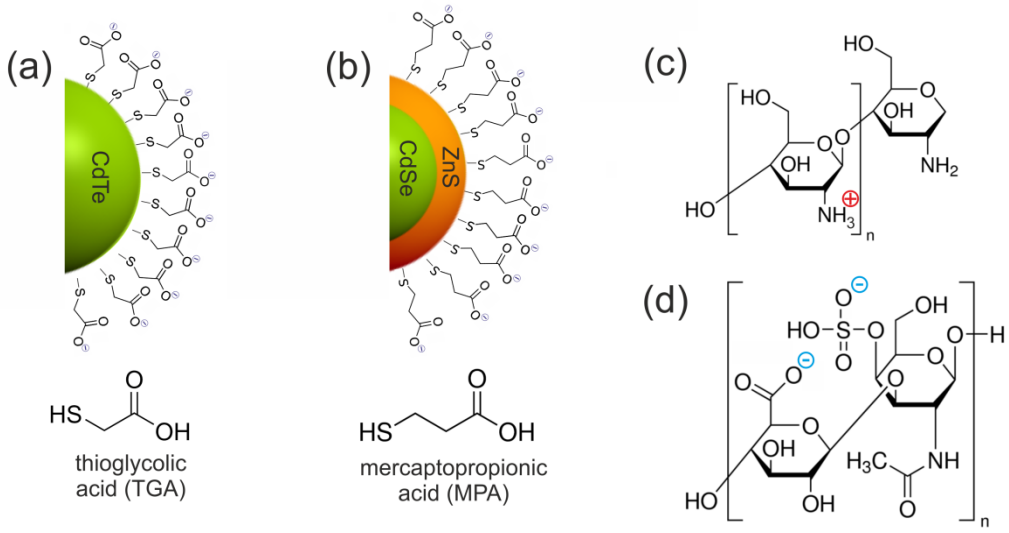

Figure 1 Structures of (a) CdTe NCs, (b) CdSe/ZnS NCs and the biopolymers: (c) chitosan; (d) chondroitin sulfate A. The charges of the species reflect their protonation/deprotonation degree under the experimental conditions of the composite synthesis.

Experimental

Materials

Water-dispersed TGA-capped CdTe and MPA-capped CdSe/ZnS nanocrystals (Fig. 1a, b) were supplied by PlasmaChem GmbH (Germany). Three different lots of each NCs types were used for the preparation of NCs-containing biopolymer particles. Hereinafter, only the reproducible results proved to be independent of the NCs prehistory will be discussed. Low-viscous (molecular weight of 420 kDa) chitosan (aminopoly-saccharide, 2-amino-2-deoxy-b-d-glucan) from shrimp shells (Fig. 1c) and sodium salts of chondroitin sulfate A [b-glucuronic acid-(1-3)-N-acetyl-b-galactosamine-4-sulfate-(1-4)] from bovine trachea (Fig. 1d) were purchased from Sigma–Aldrich and used without further purification.

Acetate buffer (pH 5.6 and ionic strength of 0.15 M) was used for the preparation of 0.1% w/v chitosan solution. Bidistilled water was used for the preparation of 0.1% w/v chondroitin sulfate solution and NCs stock (~10^{-4} M) solution. The acidity was adjusted by addition of 0.05 M aqueous solution of hydrochloric acid.

Synthesis of NCs-containing composites

The method used for the synthesis of biopolymer particles from chitosan and chondroitin sulfate was similar to that described previously.[10,11] Chitosan solution of 0.1% w/v concentration was pre-cleaned from insoluble impurities by filtration through a filter paper. The chondroitin sulfate solution of 0.1% w/v concentration was added dropwise to the chitosan solution under intensive magnetic stirring. The substances were mixed for two and a half hours. The biopolymer particles were formed as a result of self-assembly of the polycation (chitosan) and a polyanion (chondroitin sulfate). The volume ratio of chondroitin sulfate and chitosan was 1:2. The molecular polymer fraction was separated from the colloidal solution using a MiniSpin Plus centrifuge (Eppendorf, Germany) at 14,500 rpm for 5 min. After the elimination of the molecular fraction, the precipitate was ultrasonically resuspended in unbuffered solvent with pH 5.2 for 30 min. As a result, the pH-value of the solution grew up to 5.6. The concentration of biopolymer particles was about 5×10^{-4} g·ml^{-1} that agrees with the results of previous studies.[10] To obtain NCs-containing composites NCs stock solution (several gradation of volume) was added to 0.1% w/v chitosan solution prior to the mixing with the anionic component. The mixture was stirred for two hours to achieve the sorption-desorption equilibrium. The latter steps of the synthetic process were the same as for NCs-free particles. The upper boundary of the NCs content was limited by biopolymer precipitation.

Dynamic Light Scattering and ζ-Potential

The particle size distribution was derived from the dynamic light scattering data obtained by three repetitive measurements for each sample using a Delsa Nano (Beckman Coulter) device. The analysis of the autocorrelation function was carried out in approximation of solid spherical particles. ζ-Potential measurements were performed on the Zetasizer Nano ZS (Malvern Instrument, UK); each value represents an average of three repetitive runs.

Transmission electron and confocal laser scanning microscopy

Transmission electron microscope (TEM) HT7700 (Hitachi, Japan) and confocal laser scanning microscope (CLSM) LSM 780 NLO (Zeiss, Germany) were used for the visualization of NCs-containing biopolymer particles. Samples for microscopic imaging were prepared by dropping of a diluted solutions of particles onto a carbon coated copper grids (300 mesh) with a thin carbon film and glass cover slips, for TEM and CLSM studies, respectively; with subsequent drying. The samples were observed by CLSM with excitation wavelengths of 405 nm.

Steady-state and time-resolved measurements

The absorption spectra of NCs dispersed in water and NCs-containing polymer particle solution were measured on a Cary 5000i (Agilent Technologies) UV/VIS/NIR spectrophotometer equipped with an integrating sphere to eliminate scattering effects. To characterize solutions containing composites with different NCs content we used absorbance (A) at wavelength corresponding the first exciton absorption peak of NCs in assumption of a linear relationship between absorbance and average NCs concentration in the solution (regardless the embedding into a polymer particles).

The photoluminescence spectra were recorded on a Fluorolog 3-22 spectrofluorometer (Horiba Scientific) at the excitation wavelength of 400 nm. The registered signals were corrected for reabsorption, if necessary, and for sensitivity of the photomultiplier tube. The absolute PL quantum yield was obtained using Quanta-φ integrating sphere of the same manufacturer. PL measurements were carried out using a standard quartz cell (10×10 mm). The experiments were performed at room temperature.

Time-resolved measurements were performed using the DeltaHub timing module (Horiba Scientific) upon excitation with a pulsed laser diode DeltaDiode-405L with maximum at a 407 nm operating at 100 MHz with an optical pulse duration less than 55 ps. The PL lifetimes were measured near the maximum of PL spectra. The deconvolution analysis of time-resolved PL decays was carried out using DAS6 software (Horiba Scientific). The measured decay was fitted by a sum of three exponents (χ^2 was less than 1.15). In further analysis we used the average PL lifetime of NCs calculated as given by Medintz et al.[12]

Results

Morphology and ζ-potential

Chitosan and chondroitin sulfate polymers demonstrate wide multimodal size distributions (Fig. S1) at pH 5.2-5.6. However, their self-assembly due to electrostatic cross-linking results in the formation of particles with a monomodal size distribution with the maximum shifting towards larger values with the increasing of average NCs content (Fig. 2). The values of the polydispersity index were found to be similar for all the characterized samples (0.18 - 0.2) and typical for a broad size distribution of polymer particles.

CLSM and TEM images of both particle types were similar. Dried CdSe/ZnS NCs-contaning particles are shown in Fig. 3 as an example. It should be noted that the sizes of biopolymer particles determined by light scattering in aqueous solution typically exceeded the values obtained from TEM data (~100 nm), that can be explained by shrinkage of drying particles.[13] As it follows from Fig. 3b single particle can contain over a hundred NCs randomly distributed within the volume of the particle. The average distance between separate NCs depends on the NCs content and is typically comparable or bigger than the NCs size. The morphology of the obtained composites may favor their application in single-molecule spectroscopy[5,6] and FRET-based biosensors.[14]

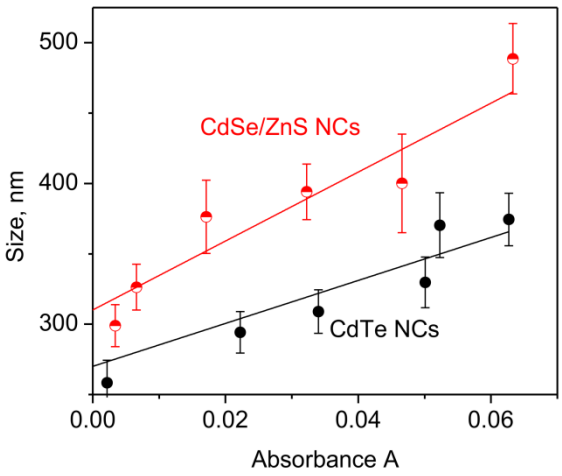

Figure 2. The dependence of polymer particles size on average NCs concentration (expressed in units of A) as determined from DLS results. The Absorbance (A) at the first exciton absorption peak is used as a unit reflecting the increasing NCs concentration.

The ζ-potential of particles was positive owing to the protonation of free amino groups of chitosan in acid media and amounted ca. +41.7 (for CdTe-containing particles) and +47.0 mV (for CdSe/ZnS-containing particles) at maximum concentration of NCs. The determined value met the requirement of electrostatic stability of the colloids.[15]

PL spectra, quantum yield and lifetime

For CdTe and CdSe/ZnS NCs dispersed in water, the first exciton absorption peaks were detected at 492 and 509 nm, the PL spectra peaks were at 529 and 526 nm, respectively (Fig. 4).

According to the size calibration for CdTe NCs dispersed in water[16] the position of the first exciton absorption peak corresponds to the NCs size of 2.4 nm. For this size the molar extinction coefficient at the first exciton absorption peak is found to be[17] 4.9×10^4 $M^{-1}\cdot cm^{-1}$. The determination of the size and the molar extinction coefficient for core-shell NCs from their spectra is challenging due to a complicated interpretation of measured data in the presence of the wide-bandgap shell. The molar extinction coefficient of CdSe NCs dispersed in water at the first exciton absorption peak was estimated as 6.2×10^4 $M^{-1}\cdot cm^{-1}$ for core size 2.4 nm.[17] The total size of CdSe/ZnS nanocrystals was defined as 3.6 nm[18] taking two monolayers of ZnS into account.

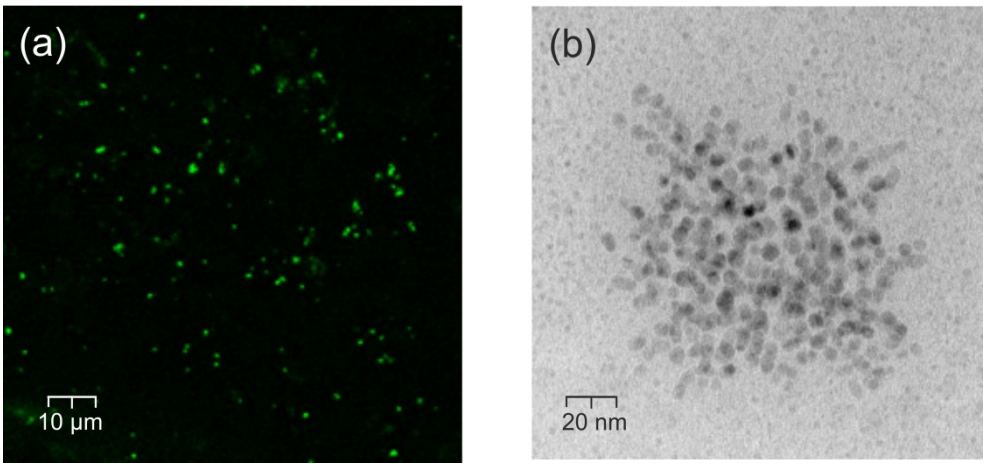

Figure 3. CLSM image of the dried CdSe/ZnS-containing particles distributed on glass cover slip (a) and TEM image of the same single particle (b).

The maximum in PL spectra of NCs embedded into polymer particles was shifted toward the red edge in comparison with NCs dispersed in water (Fig. 4). The values of the red shift amounted 2 and 12 nm for CdSe/ZnS and CdTe NCs, respectively. Similar spectral changes were reported previously for 3MPA-stabilized CdSe/ZnS NCs embedded into chitosan particles.[19] As the same spectral behavior of NCs was revealed in a 0.1% w/v aqueous (weakly acidic) chitosan solution, the spectral changes were ascribed to the binding of NCs to chitosan. The observed spectral evolution of NCs can be explained in terms of the variation of the solvent dielectric constant.[20]

Absolute values of PL quantum yield (QY) and average lifetime of CdTe NCs dispersed in water were found to be rather high amounting 51% and 36 ns respectively, whereas for CdSe/ZnS NCs these parameters amounted 47% and 19 ns respectively. The embedding of NCs into particles reduces both the values mentioned above. This effect is less pronounced for particles with a higher NCs content reflecting in the apparent growth of both the PL quantum yield and the lifetime (Fig. S2). PL quantum yield grows nearly twice whereas the relative increase of the lifetime values reaches 25-30% at the observed absorbance values.

Temporal PL properties of NCs-containing particles

The temporal stability of photoluminescence is another crucial parameter describing a luminophore along with the quantum yield. For instance, the typical duration of a complete analytical procedure such as polymerase chain reaction[21] or tumor marker tests[22] varies from several hours up to 10-15 days. In this regard, an ageing of the NCs-containing particles in the course of time was investigated. The integrated PL intensity was used for the characterization of the temporal PL stability; the measurements were performed without shaking of colloids (Fig. 5).

The solutions of polymer particles with a higher (but not the highest) CdSe/ZnS-NCs content demonstrated a significantly higher temporal PL stability revealing almost constant PL intensity within the period of 3 weeks (Fig. 5b). After this time the PL intensity decreased gradually to 65% until an abrupt drop to 10% on the 28th day. No any plateau was observed in similar graphs for CdTe-containing particles within the selected

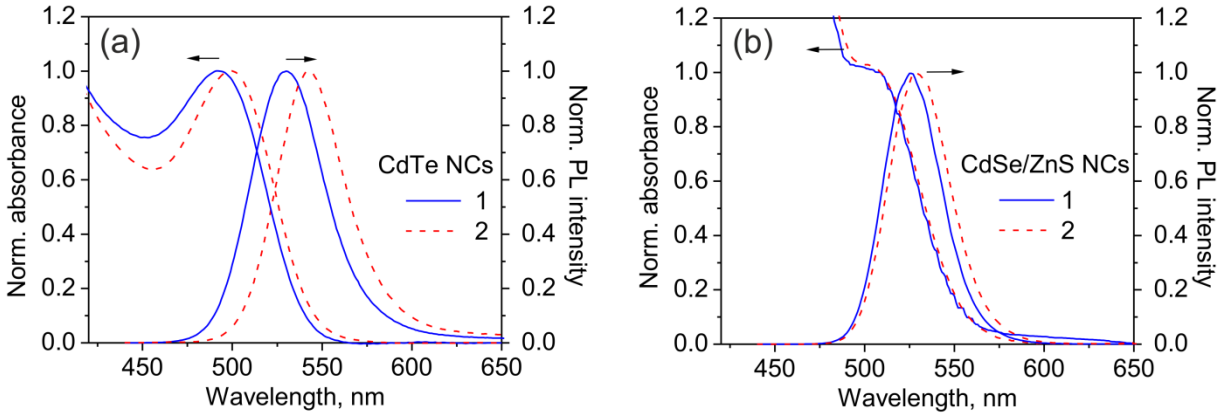

Figure 4. Absorption and PL spectra of CdTe (a) and CdSe/ZnS (b) NCs dispersed in water (1) and embedded in polymer particles (2).

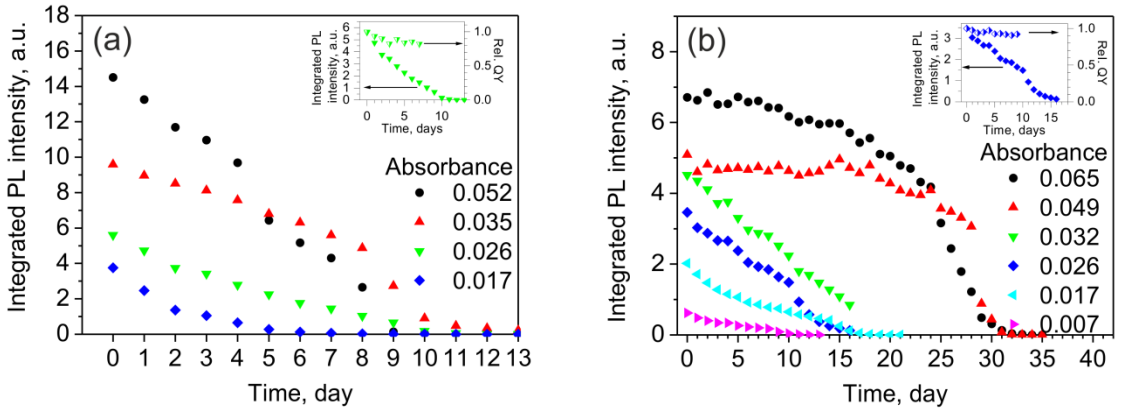

Figure 5. The temporal evolution of the integrated PL intensity of (a) CdTe- and (b) CdSe/ZnS-containing particles. The insertion shows temporal profiles of PL intensity and quantum yield (A=0.026).

range of NCs content. However even in this case the slope of the curve reciprocally depends on the NCs content.

Taking into account this behavior of PL intensity further measurements were carried out using samples with the NCs content corresponding the highest absorbance value for both types of NCs within the first 2-3 days after synthesis. The integrated PL intensity decay was accompanied by a decrease of ζ-potential of polymer particles which drops down for 7-14 mV and 5-7 mV per week for CdTe and CdSe/ZnS, respectively. The temporal evolution of the PL maximum revealed a minor blue shift for CdTe and red shift for CdSe/ZnS NCs (Fig. S3).

The value of the PL quantum yield exhibits just a very slow decrease with time whereas the integrated PL intensity drops significantly (Fig. 5, insert). It can be explained by aggregation of the NCs-containing particles resulting in the loss of their fluorescent properties and, thus, reducing the concentration of fluorophores in the colloid solution. At the same time photoluminescent properties of fluorophores (e.g., individual NCs) defining the PL quantum yield undergo minor changes only.

As distinct from the PL integrated intensity the values of the PL quantum yield of NCs-containing particles are mainly defined by the emitting properties of individual NCs. Hence, its value changes significantly slower than the PL intensity drops (Fig. 5, insert). This behavior of PL parameters can be explained by decrease of the concentration of fluorescent particles in the colloid solution, whereas photoluminescence properties of fluorophores undergo minor changes only.

Acidity effect on the optical properties of NCs-containing particles

It is well known that the acidity of the solution tremendously influences the PL properties of thiol-capped NCs.[23-28] Thus, the increasing of acid concentration results in the irreversible loss of NCs PL properties. Fig. 6 illustrates a significant decrease of the PL intensity with HCl titration of NCs dispersed in water. An abrupt PL intensity drop was observed at the HCl concentration of 1×10-4 M and 1.6×10-3 M for TGA-capped CdTe and MPA-capped CdSe/ZnS NCs, respectively.

The CdSe/ZnS NCs embedded in polymer particles do not exhibit any remarkable changes in PL intensity up to HCl concentration of 5 mM. At the same time the intensity of PL spectra of CdTe NCs gradually changed with the increase of the

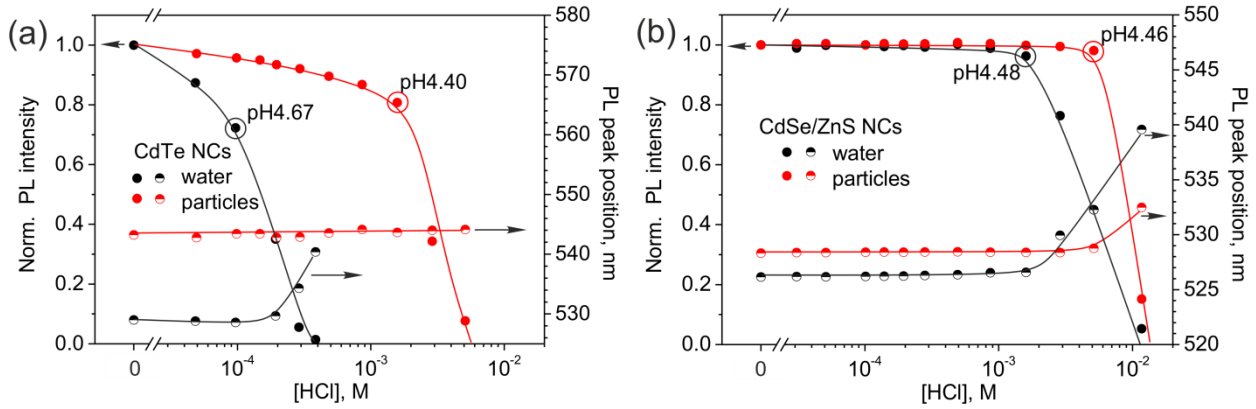

Figure 6. Dependence of the integral intensity and PL peak position of NCs dispersed in water and NCs embedded in particles on HCl concentration: (a) CdTe, (b) CdSe/ZnS.

HCl concentration up to 3 mM. Further acid addition led to a drastic decrease of the PL intensity. Nevertheless, the maximum tolerated acid concentration exceeds the critical threshold for CdTe and CdSe/ZnS NCs dispersed in water about 15 and 3 times respectively. The PL intensity drop for both NCs types was accompanied by noticeable red shifts of PL peak in all examined cases except for CdTe-containing particles (Fig. 6, S4). The measured pH values of the prepared colloid solutions significantly exceed the corresponding pH values of HCl aqueous solution with the same concentration of acid due to their buffering capacity provided by particles consisting of oppositely charged polyelectrolytes. Thus, the obtained composites maintain their photoluminescence properties even in the presence of higher amounts of acid.

Discussion

Formation of NCs-containing particles and their colloidal stability

The mechanism of the formation of NCs-free particles from chitosan and chondroitin sulfate was discussed previously.[10,11] Electrostatic linking of positively charged amino groups of chitosan with negatively charged carboxyl and sulfur groups of chondroitin (the same for hyaluronic acid and heparin[15]) plays a crucial role in the particles formation. The efficiency of the electrostatic linking is proportional to the number of charged groups determined by dissociation constants of polyelectrolytes under given conditions. Thus the value of pKa for chitosan varies within the range 6.2-6.8,[29] and amounts 3.6 for chondroitin sulfate.[30] At pH 5.6 a significant part of chitosan amino groups is protonated.

The dissociation degree β of polyelectrolytes can be described by Henderson–Hasselbalch equation establishing the correspondence between pH and β at given pK_a:

$$\mathrm{pH} = \mathrm{pK_a} + \lg\frac{\beta}{1-\beta}$$

According to this equation, the fraction of positively charged monomers of chitosan with the deacetylation degree of 85% at pH 5.6 was estimated at 68%. Thus, the concentration of positively charged monomers of chitosan in a 0.1% w/v solution amounted to about 5 mM. The maximal content of NCs (on example of CdTe NCs with *A*=0.058) was estimated as 1.2 μM.[17] Assuming the number of thiol groups on the surface of a single NC to vary from 50 to 200,[23] the calculated variation range of their concentration lies between 3.5×10^{-5} M and 1.4×10^{-4} M. The pK_a of TGA is 3.7 and MPA is 4.3,[23] therefore the dissociation degree of carboxyl groups can be assumed as almost complete (95-99%). Thus, the addition of NCs with available carboxyl groups results in their electrostatic linking to chitosan. The fraction of chitosan monomers bound to ligand lies between 1 and 3%, the rest remains positively charged (protonated).

The final stage of the formation of NCs-containing particles involves linking of the available positively charged chitosan amino groups with negatively charged carboxyl and sulfur groups of chondroitin. Considering the ionic strength,[30] the concentration of the negatively charged monomers of chondroitin sulfate was estimated as 3.2 mM that about 35% less than the concentration of the positively charged chitosan monomers. An excess of the positively charged groups taking part in the linking of two polyelectrolytes ensures the stability of the obtained colloidal solution.

Whereas the influence on the charge and, hence, the colloid stability of the obtained composites may be attributed to the varying of NCs content, an additional contribution of charged substances during the particles formation (e.g., precursors for NCs synthesis occurring in the stock solution) could shift the equilibrium toward the further protonation of chitosan amino groups. Both factors favor the colloidal stability of particles and can explain a higher colloidal stability of composites with an increased NCs content.

The most pronouncing factor responsible for the loss of the PL properties is the temporal degradation of colloidal stability resulting in the particle aggregation. In terms of the ζ-potential, the loss of the colloidal stability is reflected by the decrease of the ζ-potential below the critical value of ~30 mV.[15] After 10 days, NCs-containing particles in solution are more susceptible to attractive interparticle forces which cause them to aggregate and precipitate from solution (Fig. S5).

Acidification of the solution leads to the loss of the colloidal stability by both NCs dispersed in water and NCs-containing particles, however the latter are less sensitive and remain their PL properties within a wider range of an acid concentration. At the same time the protonation of functional groups weakens the electrostatic binding between oppositely charged polymer chains causing a 50% growth of polymer particles after swelling in 1.5 mM acid solution. Further increase of acid concentration leads to a unfolding of charged polymer chains and, finally, precipitation of polymer as the critical threshold concentration is achieved.

Changes in electronic structure of NCs

Both the ageing of composites and addition of acid to their solution result in a decrease of the PL intensity and spectral shifts. This behavior can be explained in terms of loss of the colloidal stability mainly influencing the PL intensity as well as perturbation of the band (electronic) structure of NCs responsible for the changes in the spectral profile. A monotonic decrease of the PL QY can be also related to the changes in the electronic properties of NCs (Fig. 5, insertion). Only a red shift was observed in PL spectra of NCs during the formation of composites (Fig. 4), whereas aging of NCs (Fig. S3) and acidification of the solution (Fig. S4) may result either in red or in blue shifts or have no effect on the PL peak position. We suppose that several mechanisms can contribute simultaneously to the change of the peak position in PL spectra.

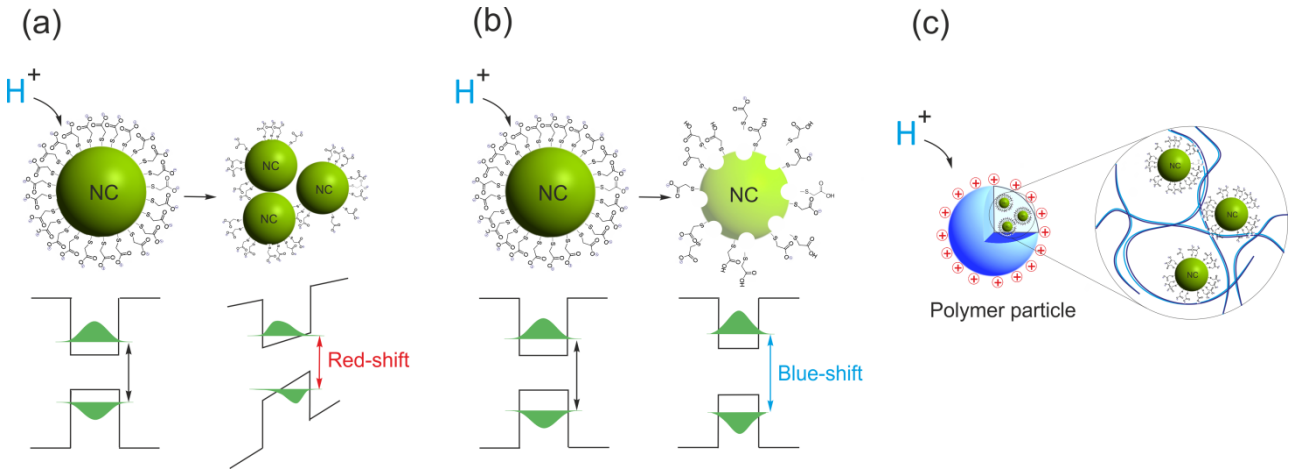

Figure 7. Schematic representation of processes influencing the PL spectral shifts (a) alteration of electric field within a near-surface range and aggregation of NCs and (b) oxidation of NCs. Frame (c) illustrates the immobilization of NCs inside the polymer particle preventing their aggregation.

One of the possible mechanisms known as quantum-confined Stark effect (QCSE)[31,32] is related to the deformation of the quantum well profile (potential barrier form) and reducing of the size-dependent quantizing energy of charge carriers. This effect is caused by the variation of the electric field strength within a near-surface region and polarizability of NCs due to their aggregation (Fig. 7a). Quantitatively the contribution of this mechanism to the PL spectrum shift (ΔE) can be represented by a term quadratically dependent on the field strength (F):

$$\Delta E = \alpha F^2$$

where α is the polarizability of the confined exciton.[33] The observed red shift of the PL peak position was accompanied by PL spectra broadening that is quite typical for the phenomenon under consideration.[33] However, any exact estimations of the role of both factors responsible for QCSE (variations of α and F) is challenging due to a complexity of the systems studied. Assuming the polarizability α as a constant (i.e., ascribing QCSE to the variation of local electric field only) it is possible to estimate the corresponding value of the electric field strength. Thus, for CdSe/ZnS NCs with α=2.01×10^{-4} meV/(kV·cm^{-1})^2 [34] revealing PL spectral shift within the range 2-10 nm in polymer particles this value lies between 70 and 150 kV·cm^{-1} that is quite typical for QCSE observed in similar systems.[31]

Another mechanism contributing PL spectral shifts is the decrease of NC size upon partial surface destruction caused by oxidation process extensively described in literature.[35] pH changes may have a significant influence on the oxidation rate.[35] The decrease of the size results in the increasing of the NC band gap and, hence, in a blue shift in the PL spectrum (Fig. 7b). The role of this mechanism is more pronounced for core-type NCs without protective shell preventing the oxidation of the core, which determines optical properties of NC. Thus, the spectra of core-shell CdSe/ZnS with a wide-gap ZnS shell NCs always exhibit QCSE-related red shift. At the same time we have not observed any red shift in PL spectra of CdTe NCs in polymer particles (a blue shift under the ageing of composites, no shift under addition of acid to their solution). Apparently, this behavior can be explained by the compensation of oxidation process and QCSE by each other.

Hence, the changes in the surrounding environment can perturb the electronic structure of NCs influencing their PL properties. The processes under consideration are mainly connected with irreversible changes on the NC surface. Immobilization in polymer particles does not provide a complete protection for NCs from oxidative destruction, however it can prevent their spontaneous aggregation (Fig. 7c) that favors the stability of PL properties in comparison with NCs dispersed in water. Therefore, unlike the CdTe in polymer particles the same NCs dispersed in water demonstrate red-shifted PL spectra related to QCSE. The similarity of the direction of spectral shifts caused by both acid addition and ageing of composites may reflect the same nature of both factors influencing the PL spectrum.

Conclusions

In summary, chitosan-based particles of 0.3-0.5 µm containing green emitting NCs of two different types (thiol-capped CdTe and CdSe/ZnS) were synthesized. Electrostatic linking of protonated chains of chitosan to the negatively charged functional groups of the NC-stabilizing ligand and to the chondroitin sulfate provided the formation of the particles at pH 5.6 without external cross-linking agents. The obtained biocompatible composites reveal a better temporal stability of photoluminescence at higher NCs content. In case of CdSe/ZnS NCs PL intensity of composites remains stable within the period of 3 weeks that meets the demands of a large number of biosensor applications.

The PL properties of the fabricated composites depend both on the band structure of NCs and colloidal stability of polymer particles. Similar changes in the PL spectra caused by aging of composites and by acidification of their solution evidence the same nature of perturbations in the electronic structure which can be explained by combination of quantum-confined Stark

effect and NCs oxidation. Immobilizing in polymer particles prevents NCs from spontaneous aggregation resulting in a better temporal stability of PL properties in comparison with NCs dispersed in water. The embedded CdTe and CdSe/ZnS NCs can sustain significantly higher concentrations of acid exceeding the maximum tolerable values for aqueous solutions of NCs for 15 and 3 times, respectively. Hence, the obtained composites extend the capabilities of thiol-capped NCs towards their application as luminescent markers for bio-imaging in acidic physiological environment.

Conflicts of interest

There are no conflicts to declare.

Acknowledgements

The reported study was particularly funded by Russian Foundation for Basic Research, Government of Krasnoyarsk Territory, Krasnoyarsk Regional Fund of Science to the research project № 18-43-242003. E. Slyusareva appreciates the Technische Universität Dresden (Germany) for the opportunity to participate in the Dresden Fellowship Program (2014-2015). The authors are grateful to the Regional Center for Collective Use of Scientific Equipment of the Tomsk State University and personally to I. Lapin for help in CLSM studies as well as to the Center for Collective Use of the Krasnoyarsk Scientific Center of the Siberian Branch of the Russian Academy of Sciences and personally to M. Volochaev for her help in TEM studies.

References

1 G. Annio, T. L. Jennings, O. Tagit and N. Hildebrandt, *Bioconjugate Chem.*, 2018, **29**, 2082-2089.
2 T. Erdem, H. V. Demir, *Nanophotonics*, 2016, **5**, 74-95.
3 G. Jin, L.-M. Jiang, D.-M. Yi, H.-Z. Sun and H.-C. Sun, *ChemPhysChem*, 2015, **16**, 3687-3694.
4 M. Stanisavljevic, S. Krizkova, M. Vaculovicova, R. Kizek and V. Adam, *Biosensors and Bioelectronics*, 2015, **74**, 562-574.
5 L. Wu, Z.-Z. Lin, H.-P. Zhong, X.-M. Chen and Z.-Y. Huang, *Sensor Actuat B-Chem.*, 2017, **239**, 69-75.
6 I. S. Osad'ko, I. Y. Eremchev and A. V. Naumov, *J. Phys. Chem. C*, 2015, **119**, 22646-22652.
7 Y. Liu, H. Oda, Y. Inoue and K. Ishihara, *Biomacromolecules*, 2016, **17**, 3986-3994.
8 A. M. Mohs, H. Duan, B. A. Kairdolf and A. M. Smith, *Nano Res.*, 2009, **2**, 500-508.
9 V. Pandey, A. Chauhan, G. Pandey and M. K. R. Mudiam, *Anal. Chem. Res.*, 2015, **5**, 21-25.
10 E. Slyusareva, M. Gerasimova, A. Plotnikov and A. Sizykh, *J. Colloid Interface Sci.*, 2014, **417**, 80-87.
11 E. Slyusareva, M. Gerasimova, V. Slabko, N. Abuzova A. Plotnikov and A. Eychmüller, *ChemPhysChem*, 2015, **16**, 3997-4003.
12 I. L. Medintz, T. Pons, K. Susumu, K. Boeneman, A. M. Dennis, D. Farrell, J. R. Deschamps, J. S. Melinger, G. Bao and H. Mattoussi, *J. Phys. Chem. C*, 2009, **113**, 18552-18561.
13 H. Dou, W. Yang, K. Tao, W. Li and K. Sun, *Langmuir*, 2010, **26**, 5022-5027.
14 M. A. Gerasimova, N. V. Slyusarenko and E. A. Slyusareva, *Proc. of SPIE*, 2017, **10614**, 106140E.
15 S. Boddohi, N. Moore, P. A. Johnson and M. J. Kipper, *Biomacromolecules*, 2009, **10**, 1402-1409.
16 A. L. Rogach, T. Franzl, T. A. Klar, J. Feldmann, N. Gaponik, V. Lesnyak, A. Shavel, A. Eychmüller, Y. P. Rakovich and J. F. Donegan, *J. Phys. Chem. C*, 2007, **111**, 14628-14637.
17 W. Yu, L. Qu, W. Guo and X. Peng, *Chem. Mater.*, 2003, **15**, 2854-2860.
18 M. Grabolle, J. Ziegler, A. Merkulov, T. Nann and U. Resch-Genger, *Ann. N.Y. Acad. Sci.*, 2008, **1130**, 235-241.
19 W. B. Tan, N. Huang and Y. Zhang, *J. Colloid Interface Sci.*, 2007, **310**, 464-470.
20 S. Xu, C. Wang and Y. Cui, *J. Mol. Struct.*, 2012, **1010**, 26-31.
21 S. Fuming, Y. Yang, Z. Hexiang, M. Meirong and Z. Zhizhou, *J. Exp. Nanosci.*, 2015, **10**, 476-482.
22 M. Fang, C. Peng, D. Pang and Y. Li, *Cancer Biol. Med.*, 2012, **9**, 151-163.
23 R. Schneider, F. Weigert, V. Lesnyak, S. Leubner, T. Lorenz, T. Behnke, A. Dubavik, J.-O. Joswig, U. Resch-Genger, N. Gaponik and A. Eychmüller, *Phys. Chem. Chem. Phys.*, 2016, **18**, 19083-19092.
24 Y. Zhang, L. Mi, P.-N. Wang, J. Ma and J.-Y. Chen, *J. Lumin.*, 2008, **128**, 1948-1951.
25 C. Maule, H. Gonçalves, C. Mendonça, P. Sampaio, J. C. Esteves da Silva and P. Jorge, *Talanta*, 2010, **80**, 1932-1938.
26 C. Wang, L. Wang and W. Yang, *J. Colloid Interface Sci.*, 2009, **333**, 749-756.
27 A. S. Susha, A. M. Javier, W. J. Parak and A. L. Rogach, *Colloids Surf. A: Physicochem. Eng. Aspects*, 2006, **281**, 40-43.
28 H. Zhang, Y. Liu, C. Wang, J. Zhang, H. Sun, M. Li and B. Yang, *ChemPhysChem*, 2008, **9**, 1309-1316.
29 R. Schmuhl, H. M. Krieg and K. Keizer, *Water S.A.*, 2001, **27**, 1-7.
30 C. Scordilis-Kelley and J. G. Osteryoung, *J. Phys. Chem.*, 1996, **100**, 797-804.
31 S. A. Empedocles and M. G. Bawendi, *Science*, 1997, **278**, 2114-2117.
32 D. Debruyne, O. Deschaume, E. Coutiño-Gonzalez, J.-P. Locquet, J. Hofkens, M. J. Van Bael and C. Bartic, *Nanotechnology*, 2015, **26**, 255703.
33 D. Braam, A. Mölleken, G. M. Prinz, C. Notthoff, M. Geller and A. Lorke, *Phys. Rev. B*, 2013, **88**, 125302.
34 S. Wu and W. Xia, *J. Appl. Phys.*, 2013, **114**, 043709.
35 A. M. Smith, H. Duan, M. N. Rhyner, G. Ruan and S. Nie, *Phys. Chem. Chem. Phys.*, 2006, **8**, 3895-3903.

